

## Visible light-induced photocatalytic performance of green MnFe<sub>2</sub>O<sub>4</sub> and CoFe<sub>2</sub>O<sub>4</sub> nanoparticles

Mohammad Lotfi<sup>1</sup>, Mortaza Mirzaei<sup>1\*</sup>, Akbar Hassanpour<sup>2</sup>, Hossein Safardoust-Hojaghan<sup>3</sup>, Ali Khani<sup>1</sup>

1. Department of Chemistry, Miyaneh Branch, Islamic Azad University, Miyaneh, Iran

2. Department of Chemistry, Marand Branch, Islamic Azad University, Marand, Iran

3. Department of Chemistry, Mashhad Branch, Islamic Azad University, Mashhad, Iran

\* Corresponding author's Email: [mortazamirzaei\\_iau@yahoo.com](mailto:mortazamirzaei_iau@yahoo.com)

### ABSTRACT

Water photocatalytic treatment has found more attention in recent years. Photocatalytic process can degrade various organic pollutants in water using free solar energy. In this study, manganese ferrite (MnFe<sub>2</sub>O<sub>4</sub>) and cobalt ferrite (CoFe<sub>2</sub>O<sub>4</sub>) as magnetic photocatalysts were prepared through novel, green and simple co-precipitation route. So, marshmallow extract was applied as green capping agent for morphological engineering of products. The crystalline structure, shape, and particle size of prepared products were characterized via X-ray powder diffraction (XRD), scanning electron microscopy (SEM), and transmission electron microscopy (TEM) techniques. The cubic phase of the products with sphere-like morphology were formed. The BET analysis revealed that the prepared MnFe<sub>2</sub>O<sub>4</sub> (72.30 m<sup>2</sup> g<sup>-1</sup>) and CoFe<sub>2</sub>O<sub>4</sub> (65.85 m<sup>2</sup> g<sup>-1</sup>) have sufficient surface area for photocatalytic application. The UV-vis diffuse reflectance spectroscopy (DRS) analysis was applied for assessment of the optical properties of these products. The optical band gap of as-obtained MnFe<sub>2</sub>O<sub>4</sub> and CoFe<sub>2</sub>O<sub>4</sub> were 2.42 and 2.71 eV, respectively. Finally, the results indicated that the MnFe<sub>2</sub>O<sub>4</sub> can removed 78, 84, and 92% of methyl orange, methylene blue, and acid violet 7 from water, after 80 min UV irradiation respectively. It was found that the photocatalytic activity of CoFe<sub>2</sub>O<sub>4</sub> is lower than MnFe<sub>2</sub>O<sub>4</sub>. Also, the further examination revealed that the photocatalytic efficiency has decreased under visible light irradiation. This study introduces MnFe<sub>2</sub>O<sub>4</sub> and CoFe<sub>2</sub>O<sub>4</sub> as excellent photocatalysts for degradation of organic pollutants.

**Keywords:** Magnetic nanomaterials, Optical properties, Photocatalyst, Surface area, Water pollutant.

**Article type:** Research Article.

### INTRODUCTION

Photocatalysis is a technology that has gained significant attention in recent years due to its ability to transform light energy into chemical one (Sakka 2013; Subramaniam *et al.* 2019). It involves using a catalyst to facilitate the conversion of light into chemical energy (Toe *et al.* 2021). Using catalysts is essential in photocatalysis, since it can enhance the efficiency of the process (Dutta *et al.* 2021; Zhu *et al.* 2021; Falih *et al.* 2022; Khadhim & Al-gubury 2023; Al-Zaidi *et al.* 2023). MnFe<sub>2</sub>O<sub>4</sub> and CoFe<sub>2</sub>O<sub>4</sub> are two of the catalysts that have been proven to be highly effective in enhancing photocatalytic activity. Manganese ferrite and cobalt ferrite are two of the most commonly used catalysts in photocatalysis (Singh & Singhal 2019; Shakir *et al.* 2021; Chaudhari *et al.* 2022; Zimur *et al.* 2023). Manganese ferrite is a type of magnetic iron oxide that has a spinel structure. It has a high surface area, which makes it an excellent candidate for enhancing photocatalytic activity (Ferreira *et al.* 2022; Manohar *et al.* 2022). Cobalt ferrite is a type of ceramic material that has a spinel structure. It is a popular catalyst in photocatalysis due to its high stability and durability (Mmelesi *et al.* 2021; Annie Vinosha *et al.* 2021). Manganese ferrite and cobalt ferrite have different physical and chemical properties. MnFe<sub>2</sub>O<sub>4</sub> has a higher surface area than cobalt ferrite, which makes it more effective in enhancing photocatalytic activity. Manganese ferrite is

also more stable than cobalt ferrite, which means that it can be reused multiple times without losing its activity.  $\text{CoFe}_2\text{O}_4$ , on the other hand, has a higher durability than manganese ferrite, which means that it can withstand harsh conditions without losing its activity (Elkholy *et al.* 2017; Miri *et al.* 2022). Manganese ferrite and cobalt ferrite have been shown to have a significant impact on photocatalytic activity. It has been found to enhance the efficiency of photocatalysis by increasing the rate of electron-hole recombination (Annie Vinosha *et al.* 2021; He & Ge 2022). This is because these ferrites have a high surface area, which provides a large number of active sites for the reaction to occur. The high surface area also allows for the adsorption of organic pollutants, which can then be degraded by the photocatalytic process (Bodaghi *et al.* 2020; Gautam *et al.* 2020).  $\text{MnFe}_2\text{O}_4$  and  $\text{CoFe}_2\text{O}_4$  have also been found to be highly effective in enhancing the degradation of dyes and other pollutants. This is due to its ability to absorb visible light, which is the most abundant source of light in the environment. The absorption of visible light by manganese ferrite results in the generation of electron-hole pairs, which can then be used to degrade the pollutants (Sharma *et al.* 2020; Shah *et al.* 2022). Manganese ferrite and cobalt ferrite have been compared with other catalysts in photocatalysis, such as titanium dioxide and zinc oxide. It has been found that manganese ferrite is more effective than these catalysts in enhancing photocatalytic activity. This is due to its high surface area and attractive magnetic behavior, which provides more active sites for the reaction to occur and facilitate to recovery and reuse (Mapossa *et al.* 2021; Annie Vinosha *et al.* 2021). Manganese ferrite is also more stable than these catalysts, which means that it can be reused multiple times without losing its activity. It is also believed that the absorption of visible light by manganese ferrite plays a significant role in enhancing photocatalytic activity. The absorption of visible light results in the generation of electron-hole pairs, which can then be used to degrade pollutants (Park *et al.* 2019; Wu & Song 2023; Mishra *et al.* 2023). The high stability of these ferrites also contributes to the enhanced photocatalytic activity, which as mentioned above, it allows for the catalyst to be reused multiple times without losing its activity (Imran Din *et al.* 2019; Kefeni & Mamba, 2020; Manohar *et al.* 2022; Ortiz-Quiñonez *et al.* 2022). The use of manganese ferrite and cobalt ferrite in photocatalysis have promising future prospects. However, there are several challenges that need to be addressed. One of the challenges is the cost of production, as manganese ferrite and cobalt ferrite are relatively expensive compared to other catalysts. Another challenge is the stability of these ferrites under harsh conditions, which needs to be improved for it to be used in industrial applications (Dutta *et al.* 2019; Ismael 2021; Bahadoran *et al.* 2022). In this work,  $\text{MnFe}_2\text{O}_4$  and  $\text{CoFe}_2\text{O}_4$  nanoparticles were synthesized through novel green chemical co-precipitation and hydrothermal routes. The structural and morphological properties of products were characterized via XRD, SEM, EDS and TEM analyses. In addition, the magnetic behavior of products was investigated via VSM analysis comprehensively. Finally, the photocatalytic activity of products were examined against different organic dyes under UV and visible light.

## **MATERIALS AND METHODS**

### **Materials**

Manganese (II) nitrate hexahydrate ( $\text{Mn}(\text{NO}_3)_2 \cdot 6\text{H}_2\text{O}$ ), iron (III) chloride hexahydrate ( $\text{Fe}(\text{NO}_3)_3 \cdot 6\text{H}_2\text{O}$ ), sodium hydroxide, ethanol and other applied chemical reagents were purchased from Merck Company.

### **Marshmallow extraction**

Marshmallow extract was provided by adding 8 g fresh marshmallow to 200 mL deionized water and then stirring it under 60 °C for 30 minutes. Finally, using a filter paper, the homogeneous solution was separated and the obtained extract was used as a capping agent for preparation of nanoparticles.

### **Green synthesis of $\text{MnFe}_2\text{O}_4$ and $\text{CoFe}_2\text{O}_4$ nanostructures**

The manganese ferrite nanoparticles was prepared via dissolving 1:2 molar ratio of  $\text{Mn}(\text{NO}_3)_2 \cdot 6\text{H}_2\text{O}$  and  $\text{Fe}(\text{NO}_3)_3 \cdot 6\text{H}_2\text{O}$  in distilled water separately. Then, 10 mL fresh marshmallow extract was added to the  $\text{Fe}^{3+}$  solution and stirred at room temperature. Afterward, the  $\text{Mn}^{2+}$  solution was mixed with  $\text{Fe}^{3+}$  and extract solution. Then NaOH (2M) solution was slightly added to the mixture and stirred for one hour. Finally, the as-obtained solid was separated by centrifugation for 10 min at 12000 rpm. Final product was obtained after drying solid at 90 °C for overnight. Finally, the dried product was heated at 900 °C for 2 h. The same chemical process was applied for preparation of cobalt ferrite nanoparticles.  $\text{Co}(\text{NO}_3)_2 \cdot 6\text{H}_2\text{O}$  and  $\text{Fe}(\text{NO}_3)_3 \cdot 6\text{H}_2\text{O}$  were applied as

precursors for preparation of  $\text{CoFe}_2\text{O}_4$  nanoparticles. Similar to the applied method for the synthesis of manganese ferrite, 5-mL fresh marshmallow extract was used for morphological engineering.

### Photocatalytic test

The synthesized  $\text{MnFe}_2\text{O}_4$  and  $\text{CoFe}_2\text{O}_4$  nanoparticles were used for the photodegradation of methylene blue, methyl orange, and acid violet 7 under UV as well as visible light at room temperature and pressure. An aliquot of  $0.005 \text{ g mL}^{-1}$  synthesized nanostructures were mixed with 30 ppm of acid violet and methylene orange solutions. The obtained mixture stirred for one hour in a dark box to provide adsorption–desorption equilibrium between the  $\text{MnFe}_2\text{O}_4$  and  $\text{CoFe}_2\text{O}_4$  nanoparticles nanostructure as well as acid violet and methylene orange. Then, the mixture was exposed to the UV and visible light and at every period of time (10 min). In addition, 5-mL organic dyes solution were filtered for recording absorbance UV-Vis spectrophotometer. The photodegradation efficiency of  $\text{MnFe}_2\text{O}_4$  and  $\text{CoFe}_2\text{O}_4$  nanoparticles was determined via the following equation (1):

$$\text{Photocatalytic efficiency \%} = \frac{C_0 - C_t}{C_0} \times 100 \quad (1)$$

where  $C_0$  is the initial concentration of dyes and  $C_t$  is the concentration after the time interval.

### RESULTS AND DISCUSSION

The X-ray diffraction (XRD) analysis was applied for determination crystallinity and structural properties of products. The XRD analysis confirmed that the synthesis of  $\text{MnFe}_2\text{O}_4$  and  $\text{CoFe}_2\text{O}_4$  nanostructures was successful and that both  $\text{MnFe}_2\text{O}_4$  and  $\text{CoFe}_2\text{O}_4$  were pure and crystalline. The presence of hematite phase in both  $\text{MnFe}_2\text{O}_4$  indicated that Fe cation has replaced Mn one in the crystalline structure of  $\text{MnFe}_2\text{O}_4$ . The peaks location confirmed formation of cubic phase of  $\text{MnFe}_2\text{O}_4$  with Fd-3m space group. Scherrer equation which was applied for determination grain size, calculated 38 nm as grain size of prepared  $\text{MnFe}_2\text{O}_4$ . In the case of  $\text{CoFe}_2\text{O}_4$ , the results confirmed formation of cubic phase with Fd-3m space group and 42.5 nm grain size. In summary, the XRD analysis provided crucial information about the composition and crystal structure of the synthesized nanostructures.

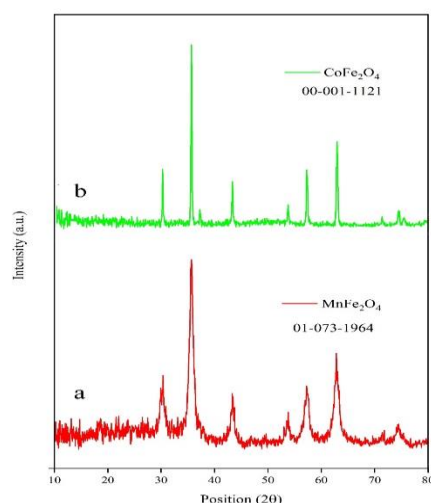


**Fig. 1.** X-ray diffraction patterns of prepared a)  $\text{MnFe}_2\text{O}_4$  b)  $\text{CoFe}_2\text{O}_4$  nanoparticles.

The SEM analysis was utilized to the studying morphological properties of products. Fig. 2a and Fig. 2b provide SEM images of prepared  $\text{MnFe}_2\text{O}_4$  nanoparticles. It can be seen from SEM images that the uniform sphere-like particles are prepared. Also, the SEM images revealed that the marshmallow extract acts as excellent capping agent. This is the advantage of this work to use green capping agent instead of chemical capping one. Fig. 2c shows the EDS analysis of prepared  $\text{MnFe}_2\text{O}_4$  nanoparticles. As shown in this Fig., the Mn, Fe, and O elements are presented in prepared nanoparticles. EDS analysis confirmed the formation of  $\text{MnFe}_2\text{O}_4$  with any impurity. Figs. 3a and 3b present SEM images of prepared  $\text{CoFe}_2\text{O}_4$  nanoparticles. It can be concluded that the uniform sphere-like  $\text{CoFe}_2\text{O}_4$  nanoparticles with average diameter of 62 nm was formed via applied green synthesis route.

The EDS analysis of obtained  $\text{CoFe}_2\text{O}_4$  nanoparticles confirmed presence of cobalt, iron, and oxygen elements in the sample. Figs. 4a and 4b provide TEM images of obtained  $\text{MnFe}_2\text{O}_4$  nanoparticles. The obtained particles size with TEM images (52 nm) is in good agreement with SEM results. Also, TEM images confirm the uniform sphere-like morphology of prepared  $\text{MnFe}_2\text{O}_4$  nanoparticles (Fig. 4).

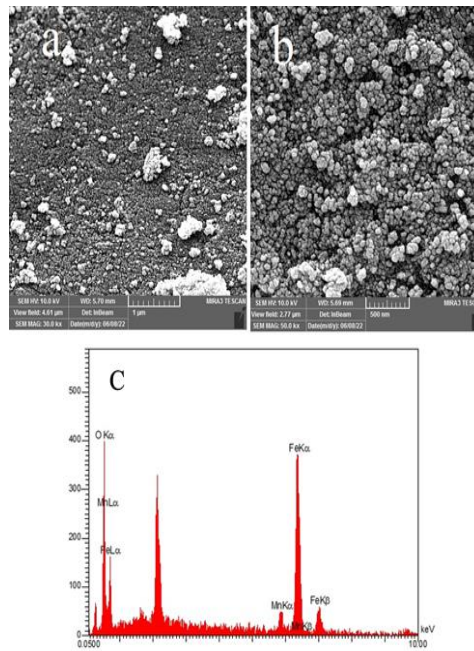


**Fig. 2.** a,b) SEM images c) EDS analysis of as-obtained  $\text{MnFe}_2\text{O}_4$  nanoparticles.

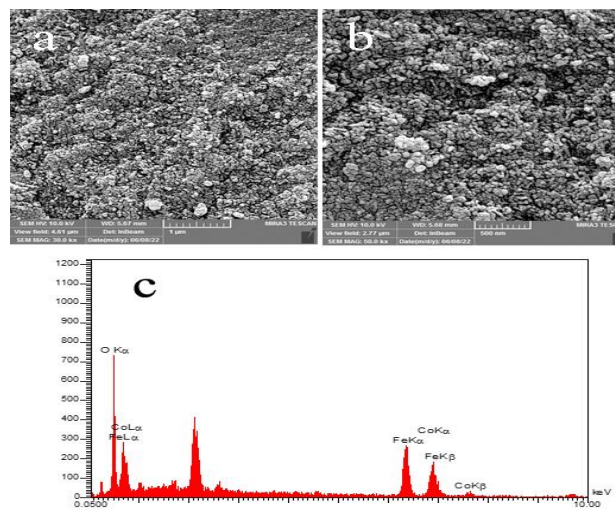


**Fig. 3.** a,b) SEM images c) EDS analysis of synthesized  $\text{CoFe}_2\text{O}_4$  nanoparticles.

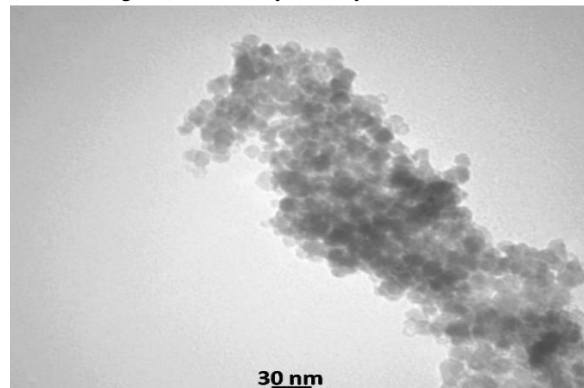


**Fig. 4.** TEM image of prepared  $\text{MnFe}_2\text{O}_4$  nanoparticles.

Manganese ferrite and cobalt ferrite are well known to show magnetic behavior that can be determined with VSM. In  $\text{MnFe}_2\text{O}_4$ , the saturation magnetization ( $M_s$ ), retentivity ( $M_r$ ), and coercivity ( $H_c$ ) were 41.50 emu/g, 2.30 emu/g and 6.76 Oe respectively (Fig. 5a). In the case of  $\text{CoFe}_2\text{O}_4$ , the saturation magnetization ( $M_s$ ), retentivity ( $M_r$ ) and coercivity ( $H_c$ ) were 49.35 emu/g, 0.64 emu/g and 7.42 Oe respectively. The obtained results are in good agreement with previously reported papers (Liu *et al.* 2021). The results suggest that the prepared ferrites possess low magnetic strength, making it suitable for applications that require weak magnetic properties like catalysis. The measurements of  $H_c$ ,  $M_r$ , and  $M_s$  are significant in comprehending the magnetic characteristics of prepared nanomaterials and can assist in advancing research and innovation in photocatalytic process (Chinnathambi *et al.* 2021).

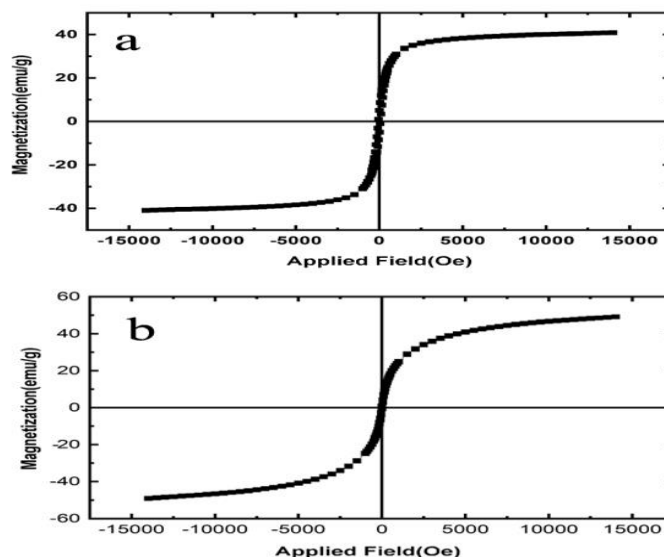


**Fig. 5.** VSM analysis of prepared a)  $\text{MnFe}_2\text{O}_4$  b)  $\text{CoFe}_2\text{O}_4$  nanoparticles.

Fig. 6a shows the manganese ferrite  $\text{N}_2$  sorption isotherm. By a type V isotherm, the isotherm displays an H3 hysteresis loop, suggesting that multilayer adsorption followed by capillary condensation exhibit in which way the adsorption of mesoporous manganese ferrite occurs. The surface area, pore volume, and pore diameter were measured  $72.30 \text{ m}^2 \text{ g}^{-1}$ ,  $0.24 \text{ cm}^3 \text{ g}^{-1}$  and  $13.39 \text{ nm}$  respectively. For  $\text{CoFe}_2\text{O}_4$ , the surface area, pore volume, and pore diameter were  $65.85 \text{ m}^2 \text{ g}^{-1}$ ,  $0.21 \text{ cm}^3 \text{ g}^{-1}$ , and  $13.28 \text{ nm}$  respectively (Fig. 6b). It can be concluded from BET analysis that the applied green capping agent leads to the synthesis of high surface area ferrites. The higher surface area of prepared nanomaterials is vital for application of nanomaterials in photocatalytic field. Optical properties of materials play key role in photocatalytic activity. So, UV-Vis-diffuse reflectance spectroscopy (DRS) was applied for investigation optical properties of prepared samples (Fig. 7a and 7c). Also, the optical band gap was calculated via Tauc equation and extrapolating the linear part of the plot of  $(\alpha h\nu)^2$  vs  $h\nu$ . In this manner, the optical band gap of synthesized manganese ferrite was  $2.42 \text{ eV}$  (Fig. 7b) while the optical band gap of obtained cobalt ferrite nanomaterials was  $2.71 \text{ eV}$  (Fig. 7d).

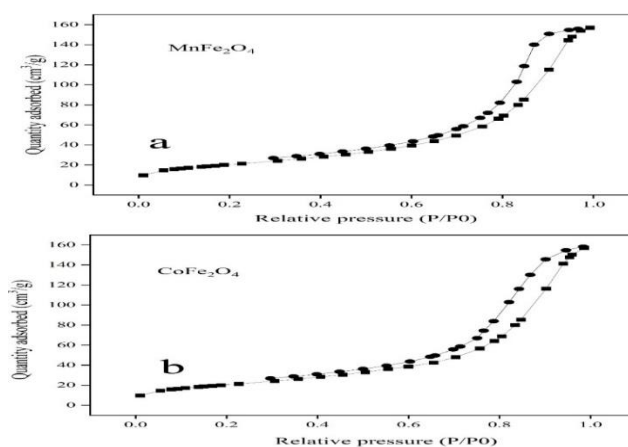


**Fig. 6.** BET analysis of synthesized a)  $\text{MnFe}_2\text{O}_4$  b)  $\text{CoFe}_2\text{O}_4$  nanoparticles.

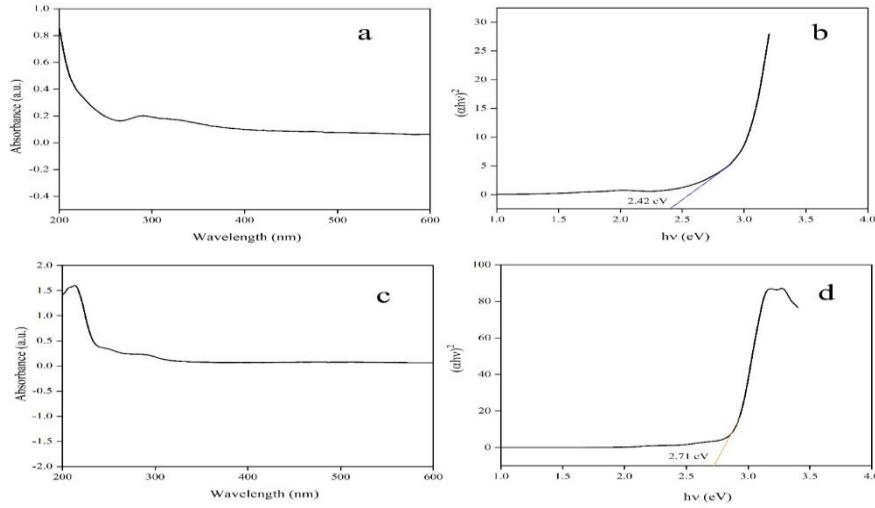


**Fig. 7.** a) DRS spectrum of MnFe<sub>2</sub>O<sub>4</sub> nanoparticles b) optical band gap of MnFe<sub>2</sub>O<sub>4</sub> nanoparticles c) DRS spectrum of CoFe<sub>2</sub>O<sub>4</sub> nanoparticles d) optical band gap of CoFe<sub>2</sub>O<sub>4</sub> nanoparticles.

The photocatalytic performance of prepared MnFe<sub>2</sub>O<sub>4</sub> and CoFe<sub>2</sub>O<sub>4</sub> was tested against methyl orange, methylene blue, and acid violet 7 dyes under UV irradiation for 80 min. The results showed that when MnFe<sub>2</sub>O<sub>4</sub> was applied as photocatalyst, it can photodegraded 78, 84, and 92% of methyl orange, methylene blue, and acid violet 7 dyes, respectively, in 80 minutes (Fig. 8). The mechanisms behind the enhanced photocatalytic activity of manganese ferrite are not yet fully understood. However, it is believed that the high surface area of manganese ferrite plays a key role in enhancing photocatalytic activity. The high surface area provides a large number of active sites for the reaction to occur, which increases the efficiency of the process. The photodegradation mechanism of manganese ferrite can be defined as:

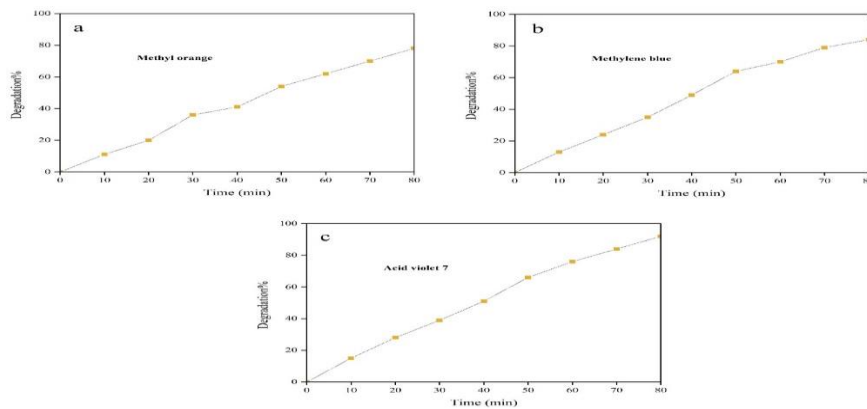
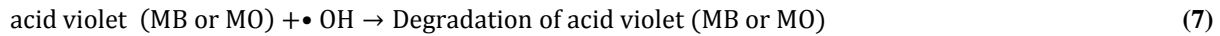
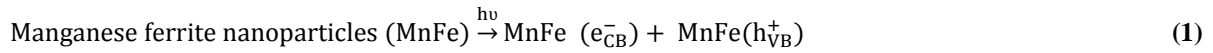


**Fig. 8.** Photocatalytic activity of prepared MnFe<sub>2</sub>O<sub>4</sub> nanoparticles against a) methyl orange b) methylene blue c) acid violet 7 under UV irradiation.

It was expected that the photocatalytic activity of CoFe<sub>2</sub>O<sub>4</sub> is lower than manganese ferrite. The result confirmed this prediction. CoFe<sub>2</sub>O<sub>4</sub> could photodegraded 72, 81, and 86% of methyl orange, methylene blue, and acid violet

7 dyes, respectively, in 80 minutes (Fig. 9). It was found that manganese ferrite is more effective than cobalt ferrite in enhancing photocatalytic activity. This is due to the higher surface area of manganese ferrite, which provides more active sites for the reaction to occur. Manganese ferrite is also more stable than cobalt ferrite, which makes it more suitable for industrial applications. The effect of irradiation light on the photocatalytic activity was investigated. The results showed that the photocatalyst under visible light has a lower efficiency compared to UV irradiation in degradation of acid violet 7. The photocatalytic efficiencies were 49 and 41% for prepared  $\text{MnFe}_2\text{O}_4$  and  $\text{CoFe}_2\text{O}_4$  nanoparticles, respectively (Fig. 10). However, these visible light-induced photodegradation are very attractive and can promise the widespread use of these nanomaterials on industrial scale.

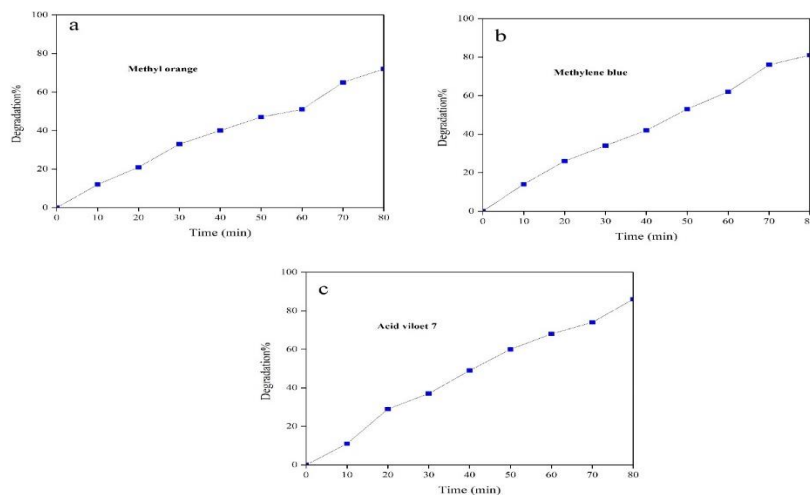


**Fig. 9.** Photocatalytic activity of prepared  $\text{CoFe}_2\text{O}_4$  nanoparticles against a) methyl orange b) methylene blue c) acid violet 7 under UV irradiation.

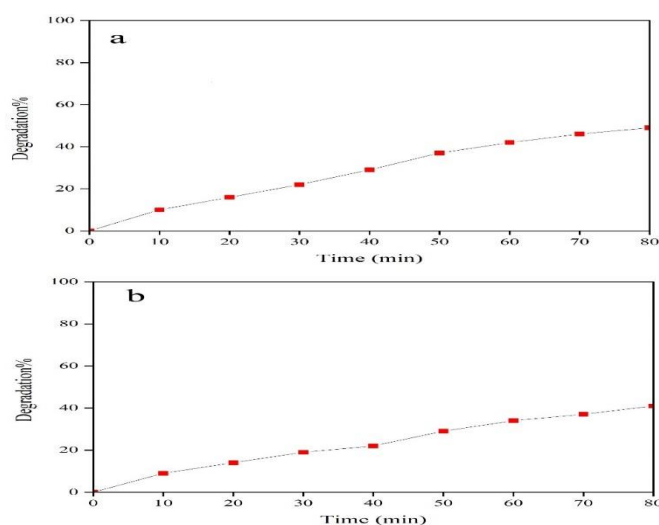


**Fig. 10.** Photocatalytic activity of prepared  $\text{MnFe}_2\text{O}_4$  nanoparticles against acid violet 7 under visible light irradiation.

## CONCLUSION

In conclusion,  $\text{MnFe}_2\text{O}_4$  and  $\text{CoFe}_2\text{O}_4$  nanomaterials were synthesized via green chemical route. The physical and chemical properties of samples were determined via SEM, TEM, XRD, and BET analyses. The results showed that marshmallow extract could act as promising capping agent for controlling shape and size of  $\text{MnFe}_2\text{O}_4$  and  $\text{CoFe}_2\text{O}_4$  nanomaterials. VSM analysis was applied for determination magnetic behavior of products. Results showed that prepared samples have excellent magnetic and morphological properties for photocatalytic application. The optical band gap of synthesized  $\text{MnFe}_2\text{O}_4$  and  $\text{CoFe}_2\text{O}_4$  were 2.42 and 2.71 eV, respectively. The photocatalytic tests showed that prepared magnetic nanomaterials can effectively photodegraded methyl orange, methylene blue, and acid violet 7 from wastewater. Also, it was found that manganese ferrite is a higher effective catalyst in enhancing photocatalytic activity rather than cobalt ferrite. It had a high surface area, which provides more active sites for the reaction to occur, and it is more stable than cobalt ferrite catalyst.

## REFERENCES

- Al-Zaidi, WJR, Ali, AM & Muhsen, TAA 2023. Efficacy of nanoparticle zinc oxide in the resistance of fungus *Rhizoctonia solani* causing black scurf disease in local potatoes. *Caspian Journal of Environmental Sciences*, 21: 95-103.
- Bahadoran, A, De Lile, JR, Masudy-Panah, S, Sadeghi, B, Li, J, Sabzalian, MH, Ramakrishna, S, Liu, Q, Cavaliere, P & Gopinathan, A 2022, Photocatalytic materials obtained from e-waste recycling: Review, techniques, critique, and update. *Journal of Manufacturing and Materials Processing*, 6: 69. <https://doi.org/https://doi.org/10.3390/jmmp6040069>.
- Bodaghi, Z, Pakpour, F & Ghanbari, D 2020, Carbon@CoFe<sub>2</sub>O<sub>4</sub>@Ag and hollow CoFe<sub>2</sub>O<sub>4</sub>@Ag nanocomposite: green synthesis of a photocatalyst and magnetic adsorbent for antibiotic removal from aqueous solutions. *Journal of Materials Science: Materials in Electronics*, 31: 19025-19035.
- Chaudhari, A, Kaida, T, Desai, HB, Ghosh, S, Bhatt, RP, & Tanna, AR 2022, Dye degradation and antimicrobial applications of manganese ferrite nanoparticles synthesized by plant extracts. *Chemical Physics Impact*, 5, 100098. <https://doi.org/https://doi.org/10.1016/j.chphi.2022.100098>.
- Chinnathambi, A, Nasif, O, Alharbi, S A, & Khan, S S 2021, Enhanced optoelectronic properties of multifunctional MnFe<sub>2</sub>O<sub>4</sub> nanorods decorated Co<sub>3</sub>O<sub>4</sub> nanoheterostructure: Photocatalytic activity and antibacterial behavior. *Materials Science in Semiconductor Processing*, 134, 105992. <https://doi.org/https://doi.org/10.1016/j.mssp.2021.105992>.
- Dutta, V, Sharma, S, Raizada, P, Hosseini-Bandegharaei, A, Gupta, VK, & Singh, P 2019, Review on augmentation in photocatalytic activity of CoFe<sub>2</sub>O<sub>4</sub> via heterojunction formation for photocatalysis of organic pollutants in water. *Journal of Saudi Chemical Society*, 23: 1119-1136. <https://doi.org/https://doi.org/10.1016/j.jscs.2019.07.003>.
- Dutta, V, Sharma, S, Raizada, P, Thakur, VK, Khan, AAP, Saini, V, Asiri, AM & Singh, P 2021, An overview on WO<sub>3</sub> based photocatalyst for environmental remediation. *Journal of Environmental Chemical Engineering*, 9: 105018. <https://doi.org/https://doi.org/10.1016/j.jece.2020.105018>.
- Elkholy, A E, El-Taib Heikal, F, & Allam, N K 2017, Nanostructured spinel manganese cobalt ferrite for high-performance supercapacitors [10.1039/C7RA11020K]. *RSC Advances*, 7(82): 51888-51895. <https://doi.org/https://doi.org/10.1039/C7RA11020K>.
- Falih, BT, Mohammed, ST & Mohammed, NJ 2022, Effects of the silver nanoparticle synthesis from the leaves of the *Capparis spinosa* plant on the liver of mice infected with visceral leishmaniasis. *Caspian Journal of Environmental Sciences*, 20: 785-791.
- Ferreira, MEC, Soletti, LdS, Bernardino, EG, Quesada, HB, Gasparotto, F, Bergamasco, R & Yamaguchi, NU 2022, Synergistic Mechanism of Photocatalysis and Photo-Fenton by Manganese Ferrite and Graphene Nanocomposite Supported on Wood Ash with Real Sunlight Irradiation. *Catalysts*, 12: 745. <https://doi.org/https://doi.org/10.3390/catal12070745>.
- Gautam, S, Agrawal, H, Thakur, M, Akbari, A, Sharda, H, Kaur, R, & Amini, M 2020, Metal oxides and metal organic frameworks for the photocatalytic degradation: A review. *Journal of Environmental Chemical Engineering*, 8: 103726. <https://doi.org/https://doi.org/10.1016/j.jece.2020.103726>.
- He, Q, & Ge, M 2022, Visible-light activation of peroxydisulfate by magnetic BiOBr/MnFe<sub>2</sub>O<sub>4</sub> nanocomposite toward degradation of tetracycline. *Journal of Materials Science: Materials in Electronics*, 33: 5859-5877. <https://doi.org/https://doi.org/10.1007/s10854-022-07768-y>.
- Imran Din, M, Rafique, F, Hussain, M S, Arslan Mehmood, H, & Waseem, S 2019, Recent developments in the synthesis and stability of metal ferrite nanoparticles. *Science progress*, 102: 61-72. <https://doi.org/https://doi.org/10.1177/0036850419826799>.
- Ismael, M 2021, Ferrites as solar photocatalytic materials and their activities in solar energy conversion and environmental protection: a review. *Solar Energy Materials and Solar Cells*, 219: 110786. <https://doi.org/https://doi.org/10.1016/j.solmat.2020.110786>.
- Kefeni, K K, & Mamba, B B 2020, Photocatalytic application of spinel ferrite nanoparticles and nanocomposites in wastewater treatment. *Sustainable Materials and Technologies*, 23: e00140. <https://doi.org/https://doi.org/10.1016/j.susmat.2019.e00140>.

- Khadhim, K & Al-gubury, HY 2023, Hydrothermal synthesis of Cr<sub>2</sub>O<sub>3</sub>/ZnO nanocomposite for environmental applications. *Caspian Journal of Environmental Sciences*, 21: 947-954.
- Liu, G, Dai, B, Ren, Y, & Zhang, W 2021, Rapid synthesis and characterization of spinel manganese ferrite nanopowder by microwave-assisted hydrothermal method. *Results in Physics*, 26: 104441. <https://doi.org/https://doi.org/10.1016/j.rinp.2021.104441>.
- Manohar, A, Vijayakanth, V, Vattikuti, SP & Kim, KH 2022, A mini-review on AFe<sub>2</sub>O<sub>4</sub> (A = Zn, Mg, Mn, Co, Cu, and Ni) nanoparticles: Photocatalytic, magnetic hyperthermia and cytotoxicity study. *Materials Chemistry and Physics*, 126117. <https://doi.org/https://doi.org/10.1016/j.matchemphys.2022.126117>.
- Mapossa, AB, Mhike, W, Adalima, JL, & Tichapondwa, S 2021, Removal of organic dyes from water and wastewater using magnetic ferrite-based titanium oxide and zinc oxide nanocomposites: a review. *Catalysts*, 11: 1543. <https://doi.org/https://doi.org/10.3390/catal11121543>.
- Miri, A, Sarani, M, Najafidoust, A, Mehrabani, M, Zadeh, FA & Varma, RS 2022, Photocatalytic performance and cytotoxic activity of green-synthesized cobalt ferrite nanoparticles. *Materials Research Bulletin*, 149: 111706. <https://doi.org/https://doi.org/10.1016/j.materresbull.2021.111706>.
- Mishra, S, Acharya, R, & Parida, K 2023, Spinel-Ferrite-Decorated Graphene-Based Nanocomposites for Enhanced Photocatalytic Detoxification of Organic Dyes in Aqueous Medium: A Review. *Water*, 15: 81. <https://doi.org/https://doi.org/10.3390/w15010081>.
- Mmelesi, OK, Masunga, N, Kuvarega, A, Nkambule, TT, Mamba, BB, & Kefeni, KK 2021, Cobalt ferrite nanoparticles and nanocomposites: Photocatalytic, antimicrobial activity and toxicity in water treatment. *Materials Science in Semiconductor Processing*, 123: 105523.
- Ortiz-Quiñonez, J-L, Das, S & Pal, U 2022, Catalytic and pseudocapacitive energy storage performance of metal (Co, Ni, Cu and Mn) ferrite nanostructures and nanocomposites. *Progress in Materials Science*, 100995.
- Park, CM, Kim, YM, Kim, KH, Wang, D, Su, C & Yoon, Y 2019, Potential utility of graphene-based nano spinel ferrites as adsorbent and photocatalyst for removing organic/inorganic contaminants from aqueous solutions: A mini review. *Chemosphere*, 221: 392-402.
- Sakka, S 2013, Chapter 11.1.2 - Sol-Gel process and applications. In S. Somiya (Ed.), *Handbook of Advanced Ceramics (Second Edition)* (pp. 883-910). Academic Press. <https://doi.org/https://doi.org/10.1016/B978-0-12-385469-8.00048-4>.
- Shah, P, Unnarkat, A, Patel, F, Shah, M & Shah, P 2022, A comprehensive review on spinel based novel catalysts for visible light assisted dye degradation. *Process Safety and Environmental Protection*, 161: 703-722. <https://doi.org/https://doi.org/10.1016/j.psep.2022.03.030>.
- Shakir, I, Agboola, PO, & Haider, S 2021, Manganese spinel ferrite-reduced graphene oxides nanocomposites for enhanced solar irradiated catalytic studies. *Ceramics International*, 47(20), 28367-28376. <https://doi.org/https://doi.org/10.1016/j.ceramint.2021.06.254>.
- Sharma, E, Thakur, V, Sangar, S & Singh, K 2020, Recent progress on heterostructures of photocatalysts for environmental remediation. *Materials Today: Proceedings*, 32: 584-593. <https://doi.org/https://doi.org/10.1016/j.matpr.2020.02.403>.
- Singh, S, & Singhal, S 2019, Transition metal doped cobalt ferrite nanoparticles: Efficient photocatalyst for photodegradation of textile dye. *Materials Today: Proceedings*, 14: 453-460. <https://doi.org/https://doi.org/10.1016/j.matpr.2019.04.168>.
- Subramaniam, MN, Goh, P-S, Lau, WJ, Ng, B-C, & Ismail, AF 2019, Chapter 3 - Development of nanomaterial-based photocatalytic membrane for organic pollutants removal. In: WJ Lau, AF, Ismail, A, Isloor & A, Al-Ahmed (Eds.), *Advanced Nanomaterials for Membrane Synthesis and its Applications* (pp. 45-67). Elsevier. <https://doi.org/https://doi.org/10.1016/B978-0-12-814503-6.00003-3>.
- Toe, C Y, Tsounis, C, Zhang, J, Masood, H, Gunawan, D, Scott, J, & Amal, R 2021, Advancing photoreforming of organics: Highlights on photocatalyst and system designs for selective oxidation reactions. *Energy & Environmental Science*, 14(3), 1140-1175. <https://doi.org/https://doi.org/10.1039/D0EE03116J>.
- Vinosh, PA, Manikandan, A, Preetha, AC, Dinesh, A, Slimani, Y, Almessiere, M, Baykal, A, Xavier, B & Nirmala, GF 2021, Review on recent advances of synthesis, magnetic properties, and water treatment applications of cobalt ferrite nanoparticles and nanocomposites. *Journal of Superconductivity and Novel Magnetism*, 34: 995-1018. <https://doi.org/https://doi.org/10.1007/s10948-021-05854-6>.

- Vinosh, PA, Manikandan, A, Preetha, AC, Dinesh, A, Slimani, Y, Almessiere, MA, Baykal, A, Xavier, B & Nirmala, GF 2021, Review on recent advances of synthesis, magnetic properties, and water treatment applications of cobalt ferrite nanoparticles and nanocomposites. *Journal of Superconductivity and Novel Magnetism*, 34: 995-1018. <https://doi.org/10.1007/s10948-021-05854-6>.
- Wu, Q, & Song, Y 2023, Recent advances in spinel ferrite-based magnetic photocatalysts for efficient degradation of organic pollutants. *Water Science and Technology*, 87(6): 1465-1495.
- Zhu, B, Cheng, B, Fan, J, Ho, W, & Yu, J 2021, g-C<sub>3</sub>N<sub>4</sub>-based 2D/2D composite heterojunction photocatalyst. *Small Structures*, 2(12), 2100086. <https://doi.org/https://doi.org/10.1002/sstr.202100086>.
- Zimur, SD, Gaikwad, P, Mali, AV, Patil, AP, Burungale, SH & Kamble, PD 2023, Magnetic and structural characterization of Sn doped cobalt ferrites; A visible light-driven photocatalysts for degradation of rhodamine-B and modeling the process by artificial intelligence tools. *Journal of Alloys and Compounds*, 947: 169572. <https://doi.org/https://doi.org/10.1016/j.jallcom.2023.169572>.